

International Shipbuilding Progress
A Study of Transom-Stern Ventilation

Lawrence J. Doctors

School of Mechanical and Manufacturing Engineering
The University of New South Wales
Sydney, NSW 2052, Australia

Gregor J. Macfarlane

Richard Young

Department of Maritime Engineering
Australian Maritime College
Launceston, TAS 7250, Australia

A STUDY OF TRANSOM-STERN VENTILATION

Lawrence J. Doctors

The University of New South Wales, Sydney, NSW 2052, Australia

Gregor J. Macfarlane

Richard Young

Australian Maritime College, Launceston, TAS 7250,

We describe here an extensive set of experiments on a series of five simplified transom-stern ship models. The local wave elevation was measured using surface transducers on the two sides of the model at the transom, as well as at the center of the transom.

This data has been analyzed and a new regression formula for the progressive ventilation of the transom, as a function of the transom-draft Froude number has been developed. These formulas take into account both the transom beam-to-draft ratio and the transom-draft Reynolds number. There is now strong evidence that the transom-draft Reynolds number plays a much lesser rôle in this phenomenon than previously thought.

Using these new formulas, one can now predict the resistance components with greater confidence. Hence, the resistance of a high-speed vessel with a transom stern can be estimated accurately over the entire speed range.

1 Introduction

1.1 Design Aspects

Many high-speed displacement or semi-displacement marine vessels are designed with transom or cutoff sterns. The reason for choosing such an apparently unstreamlined form is subject to debate.

A commonly given explanation is that this design feature allows the straightforward installation of a waterjet propulsion system in the stern of the vessel. Additionally, it is possible to make the case that the resistance of a suitably shaped transom-stern vessel can be less than that of the equivalent streamlined or sharp-ended form. Theoretical parametric resistance studies undertaken by Doctors (1999) demonstrated that an appropriate choice of the sectional area of the transom can indeed lead to this surprising outcome. It is thought that this positive result is due to the formation of the hollow in the water behind the transom, which generates a virtual extension to the length of the vessel; this creates a favorable effective Froude number based on the overall hydrodynamic length of the vessel together with the hollow.

In a series of publications, Toby (1987, 1997, and 2002) presented in-depth discussions on the desired hull form to minimize resistance. He made a similar case for the hydrodynamic advantages of a transom stern. He based his arguments on the creation of the hollow in the water and, hence, effectively increasing the wavemaking length of the vessel. He also noted the importance of the choice of the optimal size of the transom. That is, the ratio of the submerged-transom area to the maximum-section area.

A practical procedure for analyzing such high-speed and slender vessels is to employ the classic thin-ship method of Michell (1898), together with a suitable heuristic model for the transom-stern hollow. To this end, one can consult the work of Molland, Wellicome, and Couser (1994) and Couser, Wellicome, and Molland (1998). These researchers appear to be the first who developed this useful technique. This approach for modeling the transom hollow prescribed a hollow length that was invariant with the speed of the vessel. Following this effort, Doctors and Day (1997) extended the idea by means of their “firehose” model. This model ensured that the transom hollow constituted a truly continuous extension of the surface of the hull — rather akin to satisfying the Kutta condition. Furthermore, the length of the hollow increased with the speed of the vessel in a plausible manner.

1.2 Earlier Research

In the work of Doctors and Day (1997), it was assumed that the water separated completely behind the transom. That is, a fully-ventilated condition was simply modeled. As a consequence, the theoretically challenging matter of a partly-ventilated transom was not considered. It is clear that the resulting predictions for the resistance in the low-speed régime would be too high, as they observed.

A brief note in the publication of Oving (1985) seems to be one of the earliest references to the question of the partly-ventilated transom. In that report, he provided a semi-empirical formula for estimating the drop in the water level in the essentially stagnant flow region just aft of the transom. His formula yields the critical value of the transom-draft Froude number $F_T = U/\sqrt{gT}$, as a function of the beam-to-draft ratio B/T , as follows:

$$F_T^* = \begin{cases} 4.95 - 1.2B/T & \text{for } B/T \leq 2.50 \\ 1.95 & \text{for } B/T \geq 2.50 \end{cases} . \quad (1)$$

Here, U is the speed of the vessel and g is the acceleration due to gravity.

Doctors and Day (2002) tried a simple but effective approach for estimating the drop in level of the free surface immediately behind the transom stern. It was considered that the suction behind the transom was analogous to the suction that is created behind a bluff-ended body. That is, one should be able to assume a suitable pressure coefficient that is relatively independent of the transom-draft Reynolds number $R_{NT} = \sqrt{gT^3}/\nu$, in which ν is the kinematic viscosity of the water.

The elevation of the stagnant water in the hollow immediately behind the transom was then derived from the Bernoulli equation as

$$\zeta^* = C_p U^2 / 2g , \quad (2)$$

where C_p is the (negative) pressure coefficient that would be generated behind the transom stern. The hydrostatic pressure force acting on the surface of the transom stern is estimated on the basis of the *relative elevation* of the calculation point. This contribution to the resistance (positive aft) is:

$$R_{H,1} = \rho g \int_{-T^*}^{\zeta^*} b(x^*, z)(z - \zeta^*) dz , \quad (3)$$

in which ρ is the water density and T^* is the dynamic draft at the transom; this is located at the longitudinal coordinate x^* , where the local beam is $b(x^*, z)$.

Table 1: Geometric Particulars of Baby Series

Model	Length L (m)	Beam B (m)	Depth D (m)	Aft Post x_A (m)	Fwd Post x_F (m)
1	0.8000	0.1000	0.2000	0.1200	0.6000
2	0.9514	0.1189	0.2378	0.1427	0.7135
3	1.1314	0.1414	0.2828	0.1697	0.8485
4	1.3455	0.1682	0.3364	0.2018	1.0091
5	1.6000	0.2000	0.4000	0.2400	1.2000

Table 2: Test Drafts in Meters for Baby Series

Beam-to-Draft Ratio B/T	Model Number				
	1	2	3	4	5
1.000	0.1000				
1.189	0.0841	0.1000			
1.414	0.0707	0.0841	0.1000		
1.682	0.0595	0.0707	0.0841	0.1000	
2.000	0.0500	0.0595	0.0707	0.0841	0.1000
2.378		0.0500	0.0595	0.0707	0.0841
2.828			0.0500	0.0595	0.0707
3.364				0.0500	0.0595
4.000					0.0500

full description of the first set of experiments on the so-called Baby series of transom-stern ship models. The essential features of the transom flow are displayed in Figure 1(a).

Of principal interest in the current work is the measurement of the wave elevation at the center of the transom stern ζ^* . This was measured through a vertical pair of thin copper strips, closely spaced, which were glued to the center of the transom. The variation in their electrical conductivity (with changing wave elevation) was recorded by the data-logging system. It was found that this system had a very linear calibration and was quite reliable.

The wave elevation at the side of the transom ζ_S was measured in the same manner. As a check of symmetry and accuracy, these conductivity transducers were positioned on both the port and the starboard sides of the models. Thus, a total of three such probes was used. For the sake of consistency in notation, all wave elevations in this research were defined relative to the undisturbed free surface, as indicated in Figure 1(a). Therefore, the wave disturbance as measured by the probes was corrected for the measured stern sinkage of the model. The stern sinkage was determined via the vertical shift of the model as measured at the aft and the forward heave posts, using linear voltage differential transducers (LVDTs).

The parent model in the series is shown in Figure 1(b). The advantage of the rectangular stern lies in the fact that one can easily change the transom-beam-to-transom-draft ratio, while maintaining the geometric shape. This feature could be achieved, also, using a transom with an inverted triangular section, or perhaps a parabolic section. However, such shapes were considered to be less realistic in form. The dimension of all five models in the series are listed in Table 1.

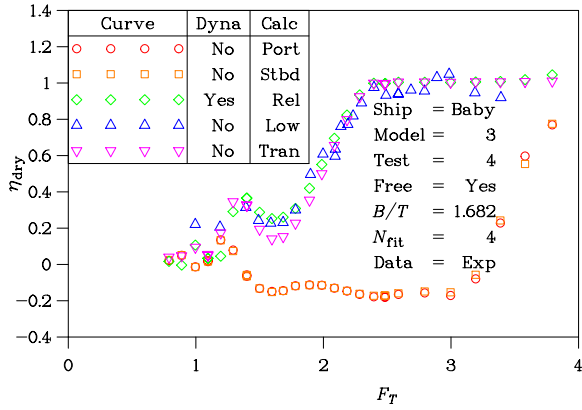


Figure 2: Ventilation of Transom
(a) $B/T = 1.682$

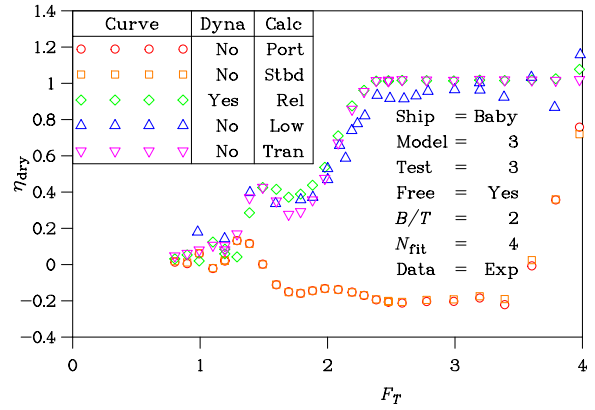


Figure 2: Ventilation of Transom
(b) $B/T = 2.000$

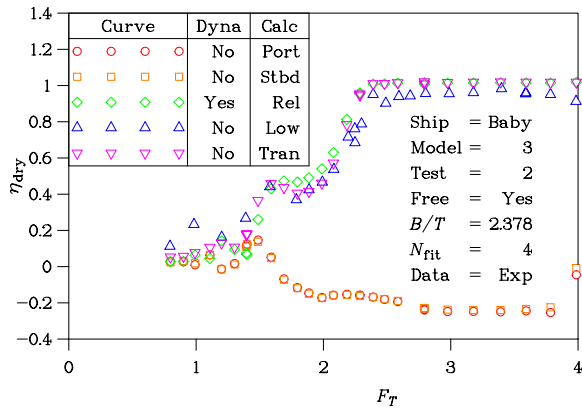


Figure 2: Ventilation of Transom
(c) $B/T = 2.378$

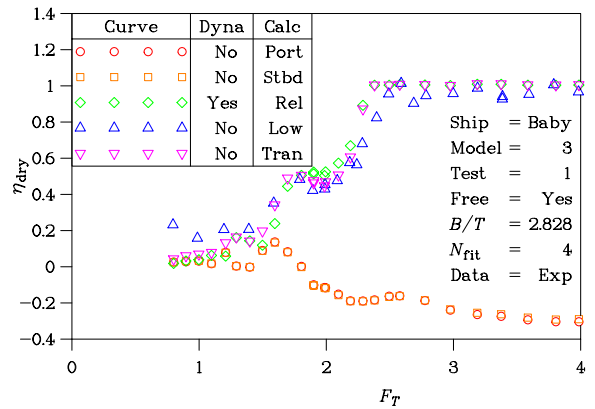


Figure 2: Ventilation of Transom
(d) $B/T = 2.828$

2.2 Tests

Each of the five models in the series was tested with five at-rest drafts, as detailed in Table 2. Because of the choice of test drafts in relation to the model dimensions, there is overlap between the data sets in that some of the values of the beam-to-draft ratio B/T were repeated. The advantage of this outcome was that repeatability of the data could be considered. Another advantage is that while the values of the beam-to-draft ratio was repeated, the transom-draft Reynolds number would be different. Hence, it was also feasible to examine the notion that “scale” could play a rôle in transom ventilation.

A range of speeds was selected, typically 25 in number, that would adequately cover the cases of interest — that is, up to speeds somewhat beyond those at which full ventilation was anticipated to occur.

2.3 Analysis

Various measures of transom ventilation have been considered. For the present work it was

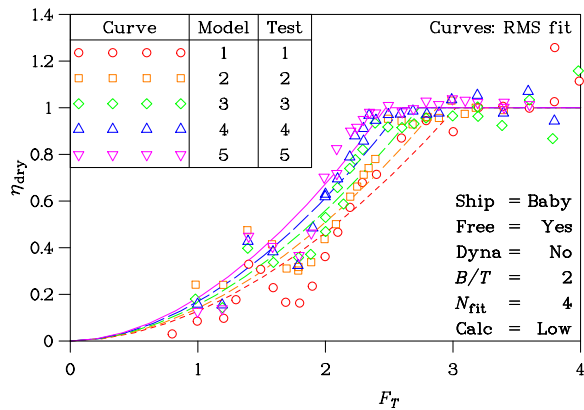


Figure 3: Influence of Reynolds Number
(a) Data from Moving Probe

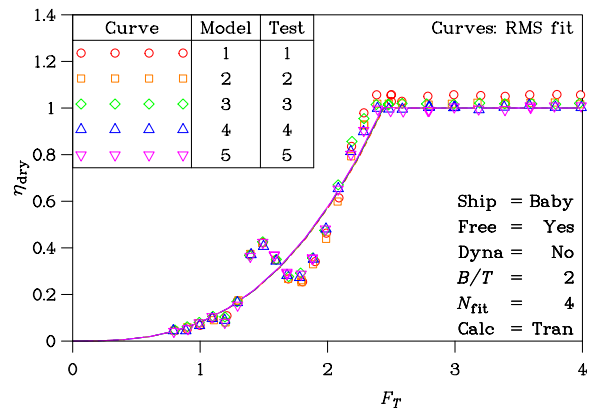


Figure 3: Influence of Reynolds Number
(b) Data from Transom Probe

decided to choose the following three parameters for evaluation and plotting:

$$\eta_{\text{dry}} = \begin{cases} -(\zeta^* + s)/T & \text{Transom ventilation ("Low" or "Tran")} \\ -(\zeta_S + s)/T & \text{Side wave elevation ("Port" or "Stbd")} \\ -(\zeta^* - \zeta_S)/(T + s + \zeta_S) & \text{Relative ventilation ("Rel")} \end{cases} . \quad (4)$$

Here, s is the sinkage of the vessel at the transom, as indicated in Figure 1(a).

The annotation “Low” refers to the data obtained from Robards and Doctors (2003), in which a longitudinally moving wave probe was used. This probe could approach the stern closely but not touch it. It was found that choosing the lowest wave elevation in the vicinity of the stern produced the most consistent analysis. The notation “Tran” refers to the transom transducer described above. The terms “Port” and “Stbd” relate to the two side transducers at the vessel stern. Finally, the abbreviation “Rel” is used to indicate the drop in the water level at the transom, relative to the vessel sides. (In the last case, the average of the port and the starboard measurements was obviously employed.)

3 Results

3.1 Ventilation of Transom

We turn to Figure 2, which shows four cases out of the total of 25 configurations detailed in Table 2. These refer to the middle Model 3 tested at four drafts. We start by considering the case of a beam-to-draft ratio B/T of 1.682 in Figure 2(a), which shows five sets of experiment data, all plotted as a function of the transom-draft Froude number F_T .

The first two sets of data are plots of the side wave elevation (port and starboard), respectively. As noted in Equation (4), these are rendered dimensionless by the vessel draft T . The plots show how there is, generally speaking, a drop in wave elevation over most of the speed range. There is also a good demonstration of the high degree of correlation between the data for the port and the starboard sides of the model, giving us confidence in the accuracy of this data.

The third set of data in Figure 2(a) indicates the relative ventilation of the transom. This data displays the characteristic increasing degree of ventilation as the speed increases, finally

Table 3: Coefficients of Transom-Ventilation Equation

Type of Analysis	Number of Coefficients	Regression Coefficients			
	N_{fit}	C_1	C_2	C_3	C_4
Moving Probe	2	0.1570	1.835		
	3	0.1559	1.830	0.01580	
	4	0.002472	1.862	0.2859	0.3588
Transom Probe	2	0.08057	2.831		
	3	0.07340	2.835	0.1247	
	4	0.06296	2.834	0.1352	0.01338

plateauing at a value of unity at the critical transom-draft Froude number F_T^* , of about 2.35. This data also displays an oscillation, illustrating a strong wave or free-surface effect. The fourth set of data was extracted from the corresponding previous experiments of Robards and Doctors (2003) and indicates the estimate of transom ventilation, computed on the basis of the lowest point in the longitudinal wave cut, close to the transom. A characteristic of this data is a certain element of randomness. This point is clear by observing that, once the transom is fully ventilated, the data does not plateau perfectly. Finally, the fifth set of data, taken from the current experiments, is seen to behave very well and plateaus to a much higher degree than the corresponding (fourth) previous set of data.

It is also worthy to emphasize that the third set of data, that for the relative ventilation, possesses a wavy characteristic which is not much less than the wavy characteristic of the fifth set of data for the transom ventilation. Thus, we can draw the conclusion, that the suction effect due to the flow of the water past the transom is somewhat more complicated than a simple application of the suction generated by the flow past a traditional backwardly-facing step in an infinite domain. That is, the concept of the “relative ventilation” has a small element of merit. However, it certainly does not explain all of the physics of transom-stern ventilation.

The other three parts of Figure 2 relate to three other transom-beam-to-transom-draft ratios. Similar comments apply to these subfigures as well.

3.2 Effects of Scale in Experiment

We now consider the matter of scale or transom-draft Reynolds number on the experiment results. This study is presented in the two parts of Figure 3. Figure 3(a) is a plot taken from the previous work of Doctors (2006).

This data is for a transom-beam-to-transom-draft ratio of 2 and was analyzed by using the low point from the moving probe, close to the transom. The five sets of data refer to the five different models. Thus, the transom-draft Reynolds number is different for each case, being greater for the larger models. This data suggests a measurable influence of the scale. In particular, it implies that the larger models ventilate faster. Naturally, the larger models would block the towing tank more. It is assumed here that this fact is not significant with regard to ventilation.

Figure 3(b) depicts the corresponding data extracted from the current experiments. It is clear that the overall effects are similar in that the ventilation process is complete at a similar transom-draft Froude number. Also, the data again displays the wave or oscillation as was evident in the earlier data of Figure 3(a). Nevertheless, there are two striking differences.

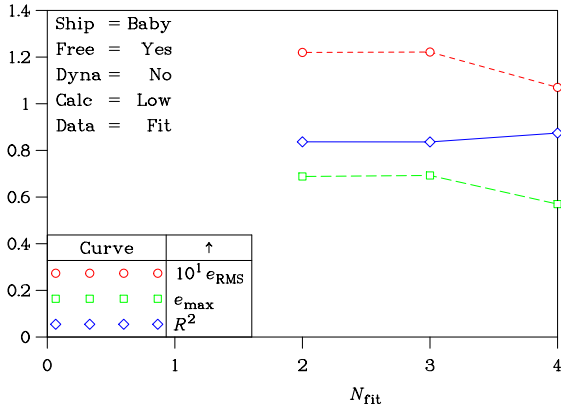


Figure 4: Convergence of Ventilation Equation (a) Data from Moving Probe

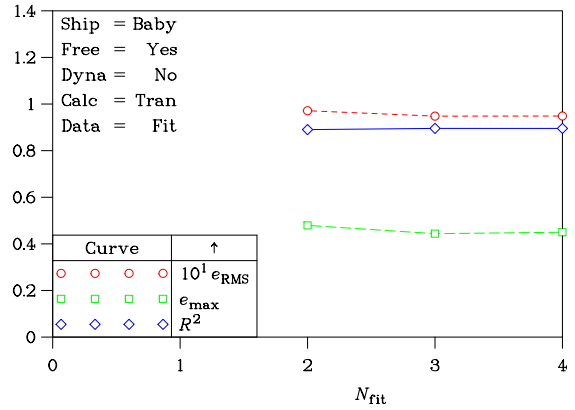


Figure 4: Convergence of Ventilation Equation (b) Data from Transom Probe

Firstly, the data for all five models now collapses almost perfectly. Thus, the data strongly implies that the influence of scale is essentially negligible. Secondly, there is very little scatter in the data; this provides a strong incentive to rely more on the newer data.

3.3 Regression Analysis

The data is presented again in numerical form in Table 3. The table is divided into two blocks. Each block contains the coefficients in the regression curve of the form:

$$\eta_{\text{dry}} = C_1 F_T^{C_2} (B/T)^{C_3} R_{NT}^{C_4}. \quad (5)$$

Both the transom-beam-to-transom-draft ratio B/T and the transom-draft Reynolds number are included in the formulation. The regression has been performed using two, three, and four coefficients, respectively.

The upper block contains the coefficients using the previous (moving-probe) data and suggests that the ventilation process is approximately proportional to $F_T^{1.84}$. The power is strongly reminiscent of the power 2 of the velocity term in the Bernoulli equation and which occurs frequently in problems of fluid dynamics. The coefficients indicate lesser effects due to the transom-beam-to-transom-draft ratio and the transom-draft Reynolds number.

The lower block in Table 3 contains the corresponding values of the four coefficients for the current (transom-transducer) data. In this case, one sees that the ventilation process is approximately proportional to $F_T^{2.83}$. This is significantly different from the result of the earlier analysis. One can also verify the almost negligible effect of the transom-draft Reynolds number (with a new power of only 0.01338). These regression curves with all factors (that is, $N_{\text{fit}} = 4$) are also plotted in the two parts of Figure 3.

The rate of convergence of the regression function with respect to the number of coefficients N_{fit} is illustrated, once again, in Figure 4. The two parts relate to both the old and the new (current) analyses. Three quantities are plotted against the number of coefficients. The curves illustrate how the root-mean-square error e_{RMS} , the maximum error e_{max} , and the correlation coefficient R^2 change, as one selects more factors in the regression equation. It is remarkable how difficult it is to improve upon the accuracy obtained with just one factor (two coefficients).

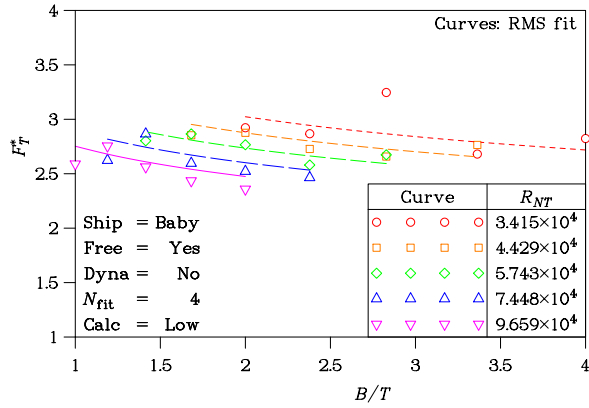


Figure 5: Critical Transom Froude Number (a) Data from Moving Probe

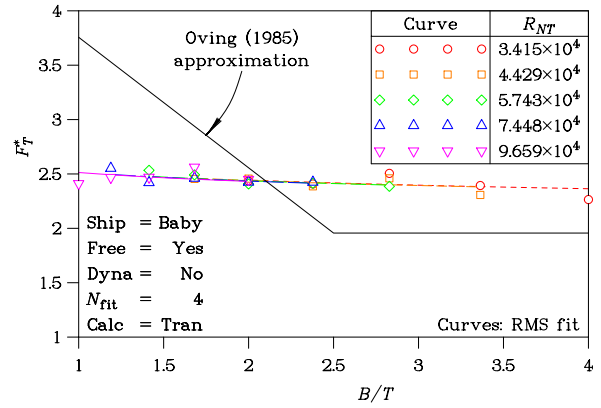


Figure 5: Critical Transom Froude Number (b) Data from Transom Probe

3.4 Critical Transom-Draft Froude Number

Finally, we show the critical transom-draft Froude number F_T^* in Figure 5. The effect of the transom-beam-to-transom-draft ratio is the key parameter of interest here. The secondary parameter is the transom-draft Reynolds number.

Figure 5(a) is a graph taken from the previous work of Doctors (2006). It is shown here for the purpose of comparison with the current work plotted in Figure 5(b). One sees that increasing the transom-beam-to-transom-draft ratio results in a lower critical transom-draft Froude number. The data also suggests (as noted above) that increasing the transom-draft Reynolds number (increasing the size of the model) advances the achievement of complete ventilation of the transom.

On the other hand, Figure 5(b) with the current analysis, indicates the almost complete absence of the influence of the transom-draft Reynolds number. Although four sets of experiment data and four corresponding regressions curve are shown on the plot, it is clear that the results all collapse nearly perfectly to a single set of data.

As a matter of further interest, we show here the curve of Oving (1985), which was reproduced above as Equation (1). There is a relatively large difference between his suggested curve of full-ventilation and our curve. On the other hand, the general effect that increasing the transom-beam-to-transom-draft ratio reduces the value of the critical transom-draft Froude number is confirmed.

4 Resistance Calculations

4.1 Components of Resistance

The primary purpose of this study is to increase our understanding of the process of the ventilation of transom sterns. An obvious benefit of this work is that we are now able to predict the transom or hydrostatic resistance with greater accuracy. To this end, we apply our knowledge to two models in the series of high-speed vessels conceived at the University of Southampton. The resistance data for these models was published by Molland, Wellicome, and Couser (1994)

Table 4: Ten University of Southampton Ship Models

Ship Model	University of Southampton Designation	Length-to-Beam Ratio L/B	Beam-to-Draft Ratio B/T	Slenderness Coefficient $L/\nabla^{1/3}$
1	3b	7.00	2.0	6.288
2	4a	10.40	1.5	7.439
3	4b	9.00	2.0	7.435
4	4c	8.00	2.5	7.404
5	5a	12.80	1.5	8.543
6	5b	11.00	2.0	8.499
7	5c	9.90	2.5	8.535
8	6a	15.10	1.5	9.538
9	6b	13.10	2.0	9.549
10	6c	11.70	2.5	9.540

and Couser, Wellicome, and Molland (1998). Pictorial views of the first two models in this series are presented in the two parts of Figure 6. Further data is listed in Table 4, where they are indicated as Model 3b and Model 4a.

Figure 7 shows the theoretical resistance components for the two chosen ship models. These components are the wave resistance R_W , the hydrostatic resistance R_H , and the frictional resistance R_F . The wave resistance was computed using the linearized theory as implemented by Sahoo and Doctors (2003). The frictional resistance was computed through the 1957 International Towing Tank Committee (ITTC) formula, described by Lewis (1988, Section 3.5).

The data is plotted as a function of the length Froude number F . The components of resistance are rendered dimensionless using the displacement weight W of the vessel. The total resistance is estimated through a simple summation of the components of resistance, as follows:

$$R_T = R_H + f_W R_W + f_F R_F. \quad (6)$$

Here, f_W is the wave-resistance form factor and f_F is the frictional-resistance form factor. For the sake of simplicity, both of these factors were chosen to be unity for the computations presented in Figure 7. The length L and the displacement Δ of the model are indicated on the graph. Also, the relative demihull centerplane spacing s/L , the relative width of the towing tank w/L and the relative water depth d/L are indicated on the plots.

One may note the increasing values of the hydrostatic resistance R_H as the speed increases, until the transom becomes fully-ventilated. The hydrostatic resistance subsequently plateaus or saturates.

4.2 Transom-Stern Flow Model

Finally, the total resistance for the two models is shown in Figure 8. For the purpose of this exercise, the contribution of the hydrostatic resistance is computed in two ways. In the first (simple) approach, the transom is assumed to be fully-ventilated at all speeds, following the work of Doctors and Day (1997). This is indicated by the symbol ‘‘Full’’. In the second approach, the drop in water level is calculated from the current regression fit to the experimental

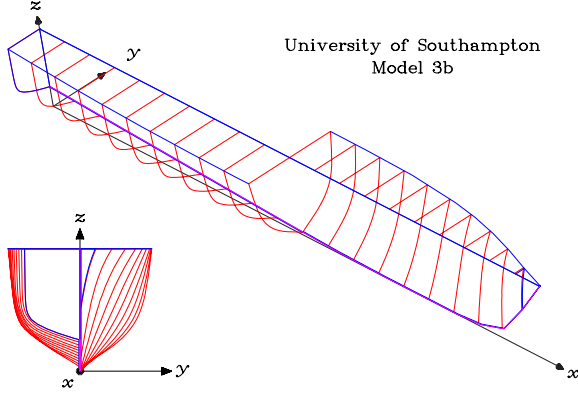


Figure 6: University of Southampton Series (a) Model 3b

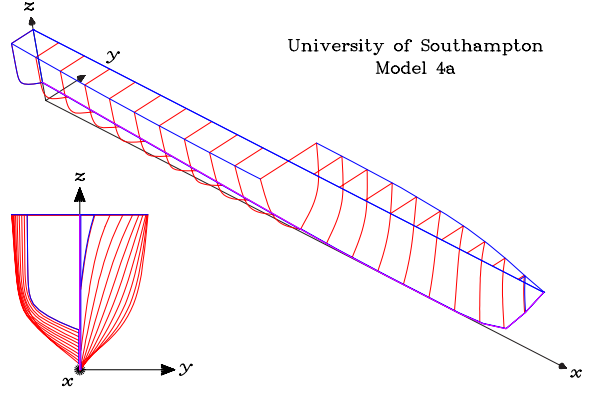


Figure 6: University of Southampton Series (b) Model 4a

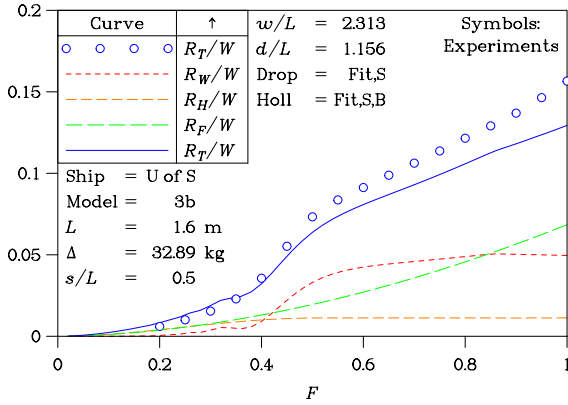


Figure 7: Components of Resistance (a) Model 3b

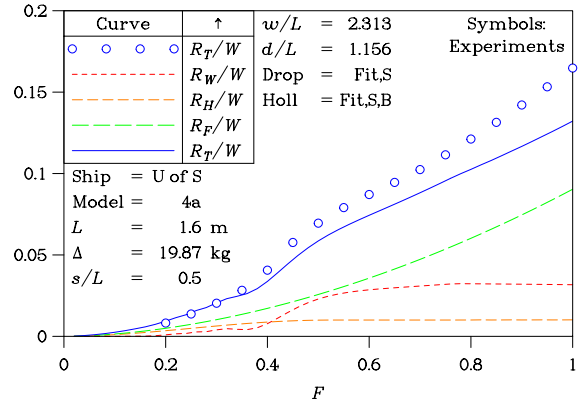


Figure 7: Components of Resistance (b) Model 4a

data according to Equation (5), using the new coefficients listed in Table 3 (derived from the analysis of the data obtained from the transom probe). This is indicated by the symbol “Fit,S”.

Regarding the estimation of the transom-stern hollow length, this was achieved using a similar approach to that for the ventilation of the transom. That is, experimental data was obtained from the experiments for the hollow and a regression fit was used. The technique was fully documented by Doctors (2006). This fact is indicated by the symbol “Fit,S,B”.

A frictional-resistance form factor $f_F = 1.000$ and a wave-resistance form factor $f_W = 1.000$ has been used for all of the theoretical calculations except for the last case, where the values $f_F = 0.9241$ and $f_W = 1.414$ have been employed. Although this value of f_F seems large, the authors have encountered this result in earlier work and similar large values have been reported by other researchers into the matter of the frictional-resistance form factor.

One can see that very good agreement for the predictions of the resistance at low values of the Froude number F is achieved using the current idealized model for the drop in water level in the transom-stern hollow region at low speeds, together with the idealized model for the growth of the hollow behind the transom stern. The chosen value of the frictional-resistance form factor

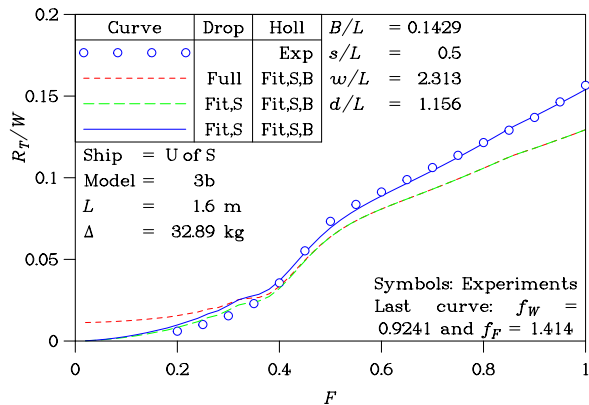


Figure 8: Transom-Stern Flow Model
(a) Model 3b

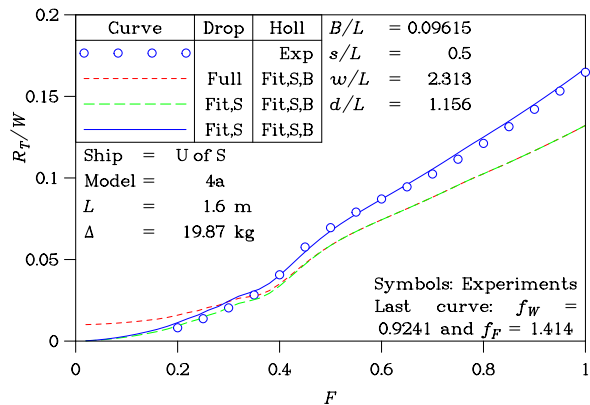


Figure 8: Transom-Stern Flow Model
(b) Model 4a

(greater than unity) was based on the entire series of ten models in this series. These choices are seen to provide a worthwhile improvement in correlation between the theory and the experiment for the total resistance R_T .

The plots of the total resistance in Figure 8 suggest little difference in the results between Model 3b and Model 4a, despite the considerable differences in geometry, as indicated in the first two entries in Table 4. This outcome is partly caused by the nondimensionalizing procedure used (the use of the specific resistance R_T/W).

Secondly, the greater frictional resistance suffered by Model 4a is compensated closely by its lesser wave resistance. This point can be verified by a careful study of the two graphs for the resistance components in Figure 7.

5 Concluding Remarks

5.1 Current Work

The current research has provided us with two new results.

The first result is that the influence of the transom-draft Reynolds number is less than that suggested by previous work on this topic. It would appear that the explanation for the difference in conclusion is that the previous experiment measurements suffered from some inaccuracy due to the need to make a correction for the self-disturbance of the moving probe.

This correction was sophisticated in that the self disturbance was carefully measured and it took into account the forward speed of the model. Additionally, account was also taken of the proximity of the probe to the transom stern, where a region of “dead water” would exist in the partly ventilated régime.

The second result relates to the concept of a relative ventilation, in which the metric is the difference in water level between that immediately behind the transom and that at the sides of the vessel. This metric can only explain the waviness in the ventilation curve to a small extent. It now appears that the free surface can affect the nature of ventilation of the transom, independently of the local elevation of the water flow at the sides of the transom.

5.2 Future Work

Work on this interesting topic can be extended in a number of directions.

The first obvious extension is to consider larger models, in order to verify that the effects of transom-draft Reynolds number are still unimportant — even on a much larger scale.

A second extension of the research would be to study transom sterns possessing different cross sections, other than the rectangular cross sections employed here.

A third extension would be to fit a ventilation function, which is more accurate than that expressed in Equation (5). The experiment data obtained during the current tests has clearly defined the wavy character of the function and it would be a bonus to employ a more precise function for the prediction of ship resistance.

6 Acknowledgments

The tests were performed in the Towing Tank at the Australian Maritime College (AMC) under the supervision of Mr Richard Young and Mr Liam Honeychurch. The theoretical analysis and the numerical calculations were performed by Professor Lawrence Doctors. The authors acknowledge the assistance of the Australian Research Council (ARC) Discovery-Projects Grant Scheme (via Grant Number DP0209656). Infrastructure support was provided by The University of New South Wales.

7 References

- COUSER, P.R., WELLICOME, J.F., AND MOLLAND, A.F.: “An Improved Method for the Theoretical Prediction of the Wave Resistance of Transom-Stern Hulls Using a Slender Body Approach”, *International Shipbuilding Progress*, Vol. 45, No. 444, pp 331–349 (December 1998)
- DOCTORS, L.J.: “On the Great Trimaran-Catamaran Debate”, *Proc. Fifth International Conference on Fast Sea Transportation (FAST '99)*, Seattle, Washington, pp 283–296 (August–September 1999)
- DOCTORS, L.J.: “Hydrodynamics of the Flow behind a Transom Stern”, *Proc. Twenty-Ninth Israel Conference on Mechanical Engineering*, Paper 20-1, Technion, Haifa, Israel, 11 pp (May 2003)
- DOCTORS, L.J.: “Influence of the Transom-Hollow Length on Wave Resistance”, *Proc. Twenty-First International Workshop on Water Waves and Floating Bodies (21 IWWF)*, Loughborough, England, 4 pp (April 2006)
- DOCTORS, L.J. AND BECK, R.F.: “The Separation of the Flow past a Transom Stern”, *Proc. First International Conference on Marine Research and Transportation (ICMRT '05)*, Ischia, Italy, 14 pp (September 2005)
- DOCTORS, L.J. AND DAY, A.H.: “Resistance Prediction for Transom-Stern Vessels”, *Proc. Fourth International Conference on Fast Sea Transportation (FAST '97)*, Sydney, Australia, Vol. 2, pp 743–750 (July 1997)
- DOCTORS, L.J. AND DAY, A.H.: “Nonlinear Free-Surface Effects on the Resistance and Squat of High-Speed Vessels with a Transom Stern”, *Proc. Twenty-Fourth Symposium on Naval Hydrodynamics*, Fukuoka, Japan, Vol. 2, pp 192–205 (July 2002)

- LEWIS, E.V. (ED.): *Principles of Naval Architecture: Volume II. Resistance, Propulsion and Vibration*, Society of Naval Architects and Marine Engineers, Jersey City, New Jersey, 327+vi pp (1988)
- MAKI, K.J., DOCTORS, L.J., BECK, R.F., AND TROESCH, A.W.: “Transom-Stern Flow for High-Speed Craft”, *Australian Journal of Mechanical Engineering*, Vol. 3, No. 2, pp 191–199 (2006)
- MICHELL, J.H.: “The Wave Resistance of a Ship”, *Philosophical Magazine*, London, Series 5, Vol. 45, pp 106–123 (1898)
- MOLLAND, A.F., WELLCOME, J.F., AND COUSER, P.R.: “Theoretical Prediction of the Wave Resistance of Slender Hull Forms in Catamaran Configurations”, University of Southampton, Department of Ship Science, Report 72, 24+i pp (March 1994)
- OVING, A.J.: “Resistance Prediction Method for Semi-Planing Catamarans with Symmetrical Demihulls”, Maritime Research Institute Netherlands (MARIN), Wageningen, 79+i pp (September 1985)
- ROBARDS, S. AND DOCTORS, L.J.: “Transom-Hollow Prediction for High-Speed Displacement Vessels”, *Proc. Seventh International Conference on Fast Sea Transportation (FAST '03)*, Ischia, Italy, Vol. 1, pp A1.19–A1.26 (October 2003)
- SAHOO, P.K. AND DOCTORS, L.J.: “A Study on Wave Resistance of High-Speed Displacement Hull Forms in Restricted Depth”, *Proc. Seventh International Conference on Fast Sea Transportation (FAST '03)*, Ischia, Italy, Vol. 1, pp A3.25–A3.32 (October 2003)
- TOBY, A.S.: “The Evolution of Round Bilge Fast Attack Craft Hull Forms”, *Naval Engineers J.*, Vol. 99, No. 6, pp 52–62 (November 1987)
- TOBY, A.S.: “U.S. High Speed Destroyers, 1919–1942: Hull Proportions (to the Edge of the Possible)”, *Naval Engineers J.*, Vol. 109, No. 3, pp 155–177, Discussion: 177–179 (May 1997)
- TOBY, A.S.: “The Edge of the Possible: U.S. High Speed Destroyers, 1919–1942. Part 2: Secondary Hull Form Parameters”, *Naval Engineers J.*, Vol. 114, No. 4, pp 55–76 (Fall 2002)